

Published in final edited form as:

Anal Bioanal Chem. 2014 January ; 406(1): 249–265. doi:10.1007/s00216-013-7446-4.

Structural features of glycol-split low-molecular-weight heparins and their heparin lyase-generated fragments

Anna Alekseeva, Benito Casu, Giuseppe Cassinelli, Marco Guerrini, Giangiacomo Torri, and Annamaria Naggi*

Ronzoni Institute for Chemical and Biochemical Research, Via Giuseppe Colombo 81, 20133 Milan, Italy

Abstract

Periodate oxidation followed by borohydride reduction converts the well-known antithrombotics heparin and low-molecular weight heparins (LMWHs) into their “glycol-split” (gs) derivatives of the “reduced oxyheparin” (RO) type, some of which are currently being developed as potential anti-cancer and anti-inflammatory drugs. Whereas the structure of gs-heparins has been recently studied, details of the more complex and more bioavailable gs-LMWHs have not been yet reported. We obtained RO derivatives of the three most common LMWHs (tinzaparin, enoxaparin, and dalteparin) and studied their structures by two-dimensional nuclear magnetic resonance (2D NMR) spectroscopy and ion-pair reversed-phase high-performance liquid chromatography (IPRP-HPLC) coupled with electrospray ionization mass spectrometry (ESI-MS). The LC-MS analysis was extended to their heparinase-generated oligosaccharides. The combined NMR/LC-MS analysis of RO-LMWHs provided evidence for glycol-splitting-induced transformations mainly involving internal nonsulfated glucuronic and iduronic acid residues (including partial hydrolysis with formation of “remnants”), and for the hydrolysis of the gs uronic acid residues when formed at the non-reducing ends (mainly, in RO-dalteparin). Evidence for minor modifications, such as ring contraction of some dalteparin internal aminosugar residues was also obtained. Unexpectedly, the *N*-sulfated 1,6-anhydro-mannosamine residues at the enoxaparin reducing end were found to be susceptible to the periodate oxidation. In addition, in tinzaparin and enoxaparin the borohydride reduction converts the hemiacetalic aminosugars at the reducing end to alditols. Typical LC-MS signatures of RO-derivatives of individual LMWH both before and after digestion with heparinases included oligosaccharides generated from the original antithrombin-binding and “linkage” regions.

Keywords

Low-molecular weight heparins; Glycol-splitting; Nuclear Magnetic Resonance; Liquid chromatography; Mass spectrometry

Introduction

Low-molecular weight heparins (LMWHs), obtained by chemical or enzymatic depolymerisation of heparin, are widely used as antithrombotic drugs [1]. They have characteristic terminal residues [2], but their linear internal sequences, like heparin, are primarily 1,4-linked trisulfated disaccharide (TSD) repeating units, containing 2-*O*-sulfated iduronic acid (I_{2S}) and *N*-sulfate-glucosamine-6-*O*-sulfate (A_{NS,6S}). These regular “fully sulfated” regions are interspersed by undersulfated sequences bearing nonsulfated iduronic

*Corresponding author: Tel. +39 0270641626; Fax +39 0270641634; naggi@ronzoni.it.

(I) and, in a somewhat higher proportion, glucuronic (G) acids, which are usually preceded by *N*-acetylated glucosamine residues (A_{NAC}). The specific pentasaccharide sequence *N*-acetyl-*D*-glucosamine-6-*O*-sulfate $\alpha 1 \rightarrow 4$ *D*-glucuronic acid $\beta 1 \rightarrow 4$ *D*-glucosamine *N*,3-*O*,6-*O*-trisulfate $\alpha 1 \rightarrow 4$ *L*-iduronic acid 2-*O*-sulfate $\alpha 1 \rightarrow 4$ *D*-glucosamine *N*,6-*O*-disulfate ($A_{NAC,6S}-G-A_{NS,3S,6S}-I_{2S}-A_{NS,6S}$), present only in some of the chains [3], constitutes the antithrombin-binding region (ATBR), essential for a high anticoagulant and antithrombotic activity of both unfractionated heparins and LMWHs.

In the last decade, several new therapeutic uses of heparins, LMWHs, and their derivatives have been envisaged in various fields [4], especially in inflammation and cancer [5–7]. To reduce risks of bleeding in non-anticoagulant/non-antithrombotic uses of heparins and LMWHs, removal or inactivation of their ATBR is required. Although removal of the ATBR-containing chains could be achieved exploiting their interaction with AT [8], a more practical way of reducing anticoagulant properties, without impairing other biological activities, is periodate oxidation of heparins [9,10]. Periodate oxidation is a classical reaction in carbohydrate chemistry that has been widely applied to determine vicinal carbons bearing unsubstituted hydroxyl and/or amino groups [11]. When applied for heparins, periodate oxidation mainly leads to the splitting of the C(2)-C(3) bond of nonsulfated uronic acids, including the essential glucuronic acid within the ATBR [12,13]. The primary products of the glycol-splitting reaction (the polyaldehydic oxy-heparins) are usually stabilized by borohydride reduction, leading to reduced oxy-heparins (RO-heparins) [9,13]. Under controlled conditions, periodate oxidation can be performed with limited cleavage of glycosidic bonds, i.e., without significant depolymerisation at the level of glycol-split (gs) residues.

The glycol-splitting reaction usually does not impair the biological activities of heparin chains that are not critically dependent on the intact structure of the AT-binding sequence. In fact, most of the literature data indicate that the glycol-splitting gives rise to a higher protein-binding activity of gs-heparins than their parent GAGs [14], most probably due to the increased local mobility of gs residues, which act as flexible joints along the polysaccharide chains, thus, facilitating interactions with the heparin/HS binding sites of proteins [7,9]. A number of non-anticoagulant gs-heparins, differing for the molecular weight and the extent of glycol-splitting, are being considered as potential antilipemic, platelet interaction-inhibiting, antithrombotic, antiangiogenic, antimetastatic, antimalarial, labor-reducing in obstetrics, and anticancer drugs [7,9,14–21]. Some of these potential drugs under development (such as, M402 [21]) were obtained from LMWHs.

The structures of a heparin [22] and a glycol-split heparin chain are depicted in Fig. 1, which also includes the “linkage region” (LR, structure 1c), i.e., the nonsulfated sequence G-Gal-Gal-Xyl, which links the carbohydrate chains with the core peptide chain of its natural proteoglycan precursor (“macromolecular heparin”) through a serine (Ser) residue [23]. The LR sequence is usually present in commercial heparins [23], however, its content and structure depends on the strength of oxidative “bleaching” treatment. Usually a few percents of intact or partially modified LR remain in heparins and in some LMWHs. G and Xyl residues, bearing vicinal hydroxyl groups, can be split. (Fig. 1d).

The structures of LMWHs are even more complex than those of their parent heparins, since both chemical and enzymatic depolymerisation of the original polysaccharide modifies the heparin sequences, at least at the site of chain cleavage, making each LMWH structurally (Fig. 2), and, to some extent biologically, different from each other [24]. Glycol-splitting and reduction reactions are expected to introduce further local modifications in LMWHs.

Pharmaceutical development of drugs of this type requires setting up appropriate analytical methods to control and guarantee preparation reproducibility and to establish correlations between structure and biological activity. Structural characterization of heparin species largely relies on NMR and/or LC-MS analysis, with the latter most often performed on fragments [25]. Significant advances in the analysis of heparin/heparan sulfate di- and oligosaccharides have been achieved by coupling ion-pair reversed-phase high-performance liquid chromatography (IPRP-HPLC) with electrospray ionization mass spectrometry (ESI-MS) [13,26–30]. However, as with heparins, one major problem in the analysis of gs-heparins is associated with their structural microheterogeneity, which can be unravelled only through careful cleavage of their chains and identification of the generated di- and oligosaccharide fragments. Glycol-splitting followed by enzymatic digestion with a cocktail of heparinases (heparin lyases I, II and/or III) has been recently used for structural characterization of heparins of different origins [13]. Heparin lyases preferentially cleave glycosidic bonds of heparin unmodified sequences, “skipping” disaccharide units containing gs-residues and thus generating oligosaccharides with incorporated gsG/gsl residues.

In the present study we obtained RO-derivatives of the three most common commercially available LMWHs (tinzaparin, enoxaparin, and dalteparin) and characterized their structures by heteronuclear single-quantum coherence (HSQC) NMR spectroscopy and IPRP-HPLC coupled with electrospray ionization quadrupole time-of-flight mass spectrometry (ESI-Q-TOF-MS). The resistance of oligosaccharides containing gs residues to heparinases was exploited to unravel the problem of the structural microheterogeneity and to obtain more structural information on unmodified heparin sequences.

Experimental

Reagents and starting materials

Low-molecular weight heparins were samples of commercial formulated or bulk materials of: tinzaparin sodium (Innohep, LEO Pharma, Denmark), enoxaparin sodium (Clexane, Sanofi Aventis, Italy) and dalteparin sodium (Fragmin, Pfizer, Italy), *N*-acetyl heparosan is a gift of K. Jann [31], synthetic pentasaccharide Arixtra® (fondaparinux, GSK, France). Heparin lyases I (EC4.2.2.7), II and III (EC4.2.2.8) were purchased from Grampian Enzymes, UK. Sodium periodate (>99%), dibutylamine (>99.5%), methanol (LC-MS grade), acetonitrile (LC-MS grade), acetic acid (glacial, 99.9%), formic acid (98–100%), ammonium chloride (> 99.5%) were purchased from Sigma-Aldrich, sodium borohydride (95%), from Riedel-de Haën, sodium acetate, from Merck, calcium acetate (>97%), from BDH, ethylenediaminetetraacetic acid (EDTA, >98%), from Fluka. Deionized (conductivity less than 0.06 μ S) and filtered (Millipore filter 0.22 μ m) water was used for sample dilution and for mobile phases.

Preparation of RO-derivatives

Glycol-split derivatives of tinzaparin, enoxaparin, dalteparin and *N*-acetyl heparosan (K5 polysaccharide) were prepared using the following procedure: about 40 – 50 mg of each sample were dissolved in 1.5 ml of H₂O, and 1.5 ml of 0.2 M NaIO₄ were added. The reaction mixture was left for 20 h at 4°C in the dark under stirring to avoid unspecific oxidation. The excess of periodate was neutralized by adding 200 μ l of ethylene glycol maintaining the stirring for a further hour at 4°C. Solid sodium borohydride (~ 70 mg) was added in portions to the reaction mixture and after 16 h at 4°C in the dark under stirring, the pH value was adjusted under stirring at 4°C to 7 with 5% (v/v) acetic acid. The solutions containing the gs-derivatives were desalted on a Sephadex G-10 column (80 x 2.5 cm) using water – ethanol 9:1 (v/v) as a mobile phase at 2.6 ml/min, monitoring the absorbance at 210

nm (Cary 50 UV-Vis spectrophotometer, Varian). After freeze drying, RO-samples were obtained with yields in the range of 85–92 %.

Molecular weight determination

Molecular weight determinations were performed by HP-SEC-TDA on a Viscotek (Houston, Texas) instrument equipped with a VE1121 pump, Rheodyne valve (100 μ l), and triple detector array 302 equipped with refraction index (RI), viscometer, and light-scattering (90° and 7°) systems, as described in [13]. Weight-average mean molecular mass (M_w) for RO-tinzaparin, RO-enoxaparin and RO-dalteparin were found to be 7.2, 4.7 and 6.4 kDa, respectively, somewhat lower than M_w values obtained for the parent LMWHs (7.9, 5.2 and 7.5 kDa, respectively).

Digestion with heparinases

The original and RO-LMWHs (100 μ g) were enzymatically depolymerised by heparin lyases I, II, III. The substrate (5–10 mg) was dissolved in water to obtain a 20 mg/ml solution. then 149 μ l of solution containing 50 mM sodium acetate and 5 mM calcium acetate, and 3 μ l of heparin lyases mixture (1 μ l of each lyase, 2 mU/ μ l enzyme solution) were added to 5 μ l of the substrate solution. The reaction was stirred at 37°C (Termo shaker TS-100 Biosan) for 24 h, then, stopped by adding 3 μ l of 3% formic acid. Each sample was diluted two times with water and analyzed by LC-MS.

RO-enoxaparin was digested with heparinases I, II and III also in a preparative scale for further fractionation and detailed studies by LC-MS and NMR: 175 μ l of 2 mU/ μ l solutions of each enzyme were added to a RO-enoxaparin solution (37 mg in 50 ml of a buffer containing 50 mM sodium acetate buffer and 5 mM calcium acetate). The digestion was carried out for 24 h at 37°C, and after the second addition of the enzymes (175 μ l of 2 mU/ μ l solutions of each enzyme), the reaction was maintained for further 24 h at 37°C, then, stopped by adding 1 ml of 3% formic acid. The reaction mixture was filtered using Millipore filter 3 μ m and concentrated up to 2 ml for SEC fractionation (*see next section*) and further detailed LC-MS and NMR analysis.

Preparative size-exclusion chromatography

HPLC system (Bioline Knauer S1050) was used for the size fractionation of the heparinase-digested RO-enoxaparin. 2 ml of the concentrated solution (*see the previous section*) were loaded onto the column (Superdex S30, 84 x 2 cm) and eluted with 0.25 M ammonium chloride at a flow-rate 5.0 ml/min. Based on the detection at 210 nm, seven fractions were obtained and, then, desalted on the Biofox 40/100 SEC Agarose column (89 x 3 cm) using water – ethanol 9:1 (v/v) as a mobile phase delivered at a flow-rate 15 ml/min. After concentration and freeze-drying each gs-oligosaccharide fraction was analyzed by 2D NMR and LC-MS.

Sodium borohydride reduction of the digested RO-enoxaparin fractions

The reduction of the SEC fractions of the digested RO-enoxaparin (*see the previous section*) were performed by adding of 5 μ l of 30 mg/ml solution of sodium borohydride into an aliquot (50 μ l) of 0.5 mg/ml solution of each fraction. The mixture was left at room temperature for 4 h and, then, analyzed by LC-MS.

NMR analysis

The samples (5 – 8 mg for LMWHs and RO-LMWHs, 1 – 2 mg for the isolated fractions of heparinase digest of RO-enoxaparin) were dissolved in 500 μ l of D₂O, added of 100 μ l of 10 mM solution of EDTA in D₂O, then freeze dried. 500 μ l of D₂O were added to each

lyophilized sample and the procedure of lyophilization was repeated. Spectra of the original and RO-LMWHs were recorded at 25°C on a Bruker Avance 500 MHz spectrometer (Karlsruhe, Germany), except for the fractions of the heparinase-digested RO-enoxaparin for which the NMR spectra were acquired on a Bruker Avance 600 MHz spectrometer (Karlsruhe, Germany). Both instruments were equipped with 5-mm TCI cryoprobe. Integration of peak volumes in the 2D-HSQC spectra was made using standard Bruker TOPSPIN 3.0 software. The relative content of monosaccharide residues was calculated from the corresponding anomeric cross-peaks identified by HSQC following the procedure previously applied to heparins [32] and to LMWHs [2]. HSQC spectra were obtained in phase-sensitivity enhanced pure-absorption mode with decoupling in the acquisition period (Bruker pulse program *hsqcetgpsisp.2*). Spectra were recorded using a spectral width of 8 ppm and 80 ppm in the proton and carbon dimensions, respectively. The carrier frequencies for proton and carbon were 4.7 ppm and 80 ppm. Spectra were acquired into a time domain of 1024 complex points, using from 16 to 32 scans for each of 320 increments. The repetition time and the acquisition time were set at 2s and 0.178s, respectively, with a total measurements ranging from 3h:05min up to 6h:10min. The matrix size of 1024 × 320 data points was zero filled to 4096 × 2048 by application of a squared cosine function prior to Fourier transformation. 2D-TOCSY spectra was acquired using 32 scans per series of 2048 × 512 data points and a mixing time of 80ms. A zero filling in F1 (4096 × 2048) and a shifted ($\pi/3$) squared cosine function was applied prior to Fourier transformation.

LC-MS analysis of the unmodified and RO-LMWHs and their corresponding heparinase digests

LC-MS analysis of all samples was performed on an Ultimate 3000 HPLC-UV system (Dionex) coupled to an ESI-QTOF mass spectrometer MicrOTOF-Q (Bruker Daltonics, Germany). Ion-pair reversed-phase separation was carried out on a Kinetex-C18 column (2.1 × 100 mm, ODS 2.6 μm , 100 Å, Phenomenex) with Security Guard Cartridges Gemini C18 (4 × 2.0 mm, Phenomenex). A binary solvent system was used for gradient elution.

LC-MS analysis of the heparinase-digested original and RO-LMWHs was performed as previously described in [13]. For profiling the intact unmodified LMWHs and RO-LMWHs, methanol in the mobile phases, used for the analysis of the enzymatic digests [13], was substituted by acetonitrile. This substitution led to a decrease in column backpressure and, consequently, permitted an increase in the flow-rate (from 100 up to 250 $\mu\text{l}/\text{min}$), which resulted in a decrease of total analysis time, and, more important, improved chromatographic performance. Thus, for profiling the non-digested original and RO-LMWHs, mobile phases A (10 mM dibutylamine, 10 mM acetic acid in water – acetonitrile (9:1)) and B (10 mM dibutylamine and 10 mM acetic acid in acetonitrile), delivered at 0.25 ml/min, were used. Because enoxaparin, tinzaparin and dalteparin are characterized by a different molecular weight distribution, slightly different multistep gradients were used for their profiling (Table 1). Under the applied conditions the retention times vary in a range 1.0 – 1.5 %.

The MS spectrometric conditions were as follows: ESI in negative ion mode, drying gas temperature +180°C, drying gas flow-rate 7.0 l/min, nebulizer pressure 0.9 bar, capillary voltage +3.2 kV. The mass spectra of the oligosaccharides were acquired in a scan mode (m/z scan range 200 – 2000). The fragmentation of the ion with m/z 488.5, present in the digested RO-enoxaparin, was performed by applying LC-ESI-MS² method. Collision-induced dissociation (CID) was used, the isolation window was set at 5 Da and the collision energy was –20 eV.

Nomenclature and structure identification

In the present work the abbreviation RO is used for describing the samples obtained by glycol-splitting followed by the reduction to highlight this latter step, while gs is used to indicate the split units within RO-LMWHs chains.

The oligosaccharide identification was based on the MS data. Their formula was only accepted if the m/z of the candidate analyte matched with the theoretical value within 5 ppm for oligosaccharides up to dp 8. For higher chain length oligosaccharides an error within 10 ppm was accepted. The comparison of the experimentally obtained isotope pattern with the theoretical one was also used to confirm the assigned structure. For each peak a “first-level structure” was assigned using MS data and considering the chemical nature and treatments of the starting material. The nomenclature previously applied for the heparinase-digested RO-heparins [13] was used. The abbreviation system is similar to that of Henriksen et al [33] and includes the number of monosaccharide residues, sulfate groups, and *N*-acetyl groups. In our case, a number and the symbol gs were also added to indicate the number of the glycol-split residues. “Remnants” of the hydrolyzed internal gs residues were indicated by the symbol R (see Fig. 1e), and those from non-reducing end as R(Unr), respectively. Symbols ΔU, U and A indicate a 4,5-unsaturated uronic acid, a saturated one and a glucosamine unit, respectively, at the NRE. Symbol “ol” indicates the alditol form of terminal units at the RE; symbols aM.ol and Rc indicates 2,5-anhydromannitol and contracted ring residues typical for dalteparin. Symbols 1,6aA and 1,6aM were used for the NMR cross peaks of 1,6-anhydroglucosamine and 1,6-anhydromannosamine units typical for enoxaparin; while for LC-MS data 1,6aA was used for both epimers because it was not possible to distinguish them from MS data.

Results

NMR analysis of RO-LMWHs

In order to detect and quantify monosaccharidic residues and units of LMWHs affected by the glycol-splitting reaction, RO-LMWHs were analyzed by 2D-NMR spectroscopy, using the $^1\text{H}/^{13}\text{C}$ HSQC approach previously developed for the structural characterization of unmodified heparins [32] and LMWHs [2]. The HSQC spectra of heparin species consist of a characteristic series of spots (cross peaks) over the typical range of monodimensional ^1H and ^{13}C spectra, the most informative for the current purpose usually being in the region of the anomeric (H-1/C-1) protons and carbons (5.6–5.4 / 94–108 ppm, including the small region of unsaturated ^1H and ^{13}C at 6.0-5.8/108–111 ppm), which is regarded as the “structural reporter” region of the spectra. As indicated in Fig. 3 for tinzaparin (blue spots) and RO-tinzaparin (red spots), signals for typical residues are located in subregions of the spectrum. Disappearance of cross peaks associated with residues known to be susceptible to periodate/borohydride reactions as indicated in Fig. 1 and 2, and appearance of new ones, with slight perturbation of cross peaks, clearly attributable to residues that are unaffected by these reactions, are evident in Fig. 3, Fig. S1 and S2 (see Electronic Supplementary Material.). Chemical shifts associated with gs-residues in different heparin-related compounds (heparins, LMWHs and K5PS) are listed in Table 2. Table S1 (see Electronic Supplementary Material) reports the relative content of typical residues for the three prepared RO-LMWH samples measured from the signal volumes [2,32].

As expected, for all the three LMWHs the strongest signals are those that are less affected by glycol-splitting, i.e., those of the internal “regular” sequences of the trisulfated disaccharide (TSD) $\text{I}_{2\text{S}}\text{-A}_{\text{NS6\text{S}}}$ [32] Distinct spots are associated with G-, gsG- and A_{NAC^-} -containing disaccharide sequences (5.0-4.5/108-104 ppm). The H-1/C-1 signals most typical for the gs residues (at 4.98/106.9 ppm and at 4.80-4.87/106.4 ppm) are at positions similar to

those that we recently identified for gsI and gsG, respectively, in RO-heparins [13,14]. Notably, cross-peak G-(A*) at 4.62/103.9 ppm, taken as a marker of the ATBR [34], is common to the three unmodified LMWHs but disappears upon glycol-splitting. The corresponding gsG-(A*) signal (at 4.90/103.2) was identified in RO-LMWHs. Such an assignment was confirmed by TOCSY experiments (see Electronic Supplementary Material, Fig. S3), indicating a correlation of the signal with CH₂OH signals of a gsU residues. Moreover, cross peaks with similar chemical shifts were found in the spectrum of the RO-derivative of the synthetic pentasaccharide AGA*IA (4.94/103.4 ppm) and in that (4.98/103.1 ppm) of the RO-derivative of a heparin fraction enriched in ATBR-containing chains obtained by affinity chromatography [13] (data not shown). Signal gsG-(A*) is clearly observed only in the spectrum of RO-dalteparin (see Electronic Supplementary Material, Fig. S2), but can be also detected in the expanded scale spectrum of the other RO-LMWHs. It is thought that different contents of the glycol-split ATBR disaccharide largely reflect different contents of G-(A*) in the original LMWHs as reported in the Table S1 (see Electronic Supplementary Material). Together with these signals from “internal” gsI and gsG, at least one cross peak (at 4.92/107.6), typical for RO-heparin species containing the linkage region, can be assigned to the glycol-split G residue (gsG_{LR}) preceding the first galactose residue (Gal1). As in the spectra of the parent LMWHs, the gsG_{LR} signal intensity indicates that the content of LR in RO-tinzaparin is consistently higher than in RO-enoxaparin, while that in RO-dalteparin is very low, the corresponding signal not being observed in spectrum (see Electronic Supplementary Material, Fig. S2).

NMR data (Fig. 3) show that not only internal sequences but also several end-groups are susceptible to glycol-splitting and/or reduction. For example, the cross-peaks of both α and β anomers of aminosugars and uronic acids at the RE typical for unmodified tinzaparin ($A_{NS\alpha}$, $A_{NS\beta}$, Fig. 3) and enoxaparin ($A_{NS\alpha}$, $A_{NS\beta}$, $M_{NS\alpha}$, $M_{NS\beta}$, $I_{2S\alpha}$, $I_{2S\beta}$, see Fig. S1 of the Electronic Supplementary Material) disappeared after the RO-reaction. The resulting RE-alditols are not detectable in the complex “ring region” of the NMR spectra due to the signal overlapping with the free primary hydroxyl groups at C-6 of glucosamine and those at C-2 and C-3 of gs-uronic acids (Fig. 3, Fig. S1). The enoxaparin cross-peaks of H4/C4 Δ U and those of H1/C1 in 1,6aM are among those that disappear upon periodate oxidation/borohydride reduction (See Discussion). The NMR spectrum of dalteparin confirms its relative structural homogeneity, with a 2-*O*-sulfated iduronic acid at the NRE and a 2,5-anhydromannitol (aM.ol) at the RE, this latter residue well identifiable in the “ring region” of the NMR spectrum (see Electronic Supplementary Material, Fig. S2). A weak signal at 5.45/104.5 ppm in both dalteparin and RO-dalteparin was recognized and assigned for the first time to an internal glucosamine contracted ring (Rc) residue using homonuclear (1D-COSY and 1D-TOCSY) and heteronuclear (edited-HSQC and HSQC-TOCSY) experiments (Electronic Supplementary Material Fig. S4). Particularly, the intra-residue connections were obtained starting from the 2-C-hydroxymethyl signal at 2.53 ppm, not affected by signal overlapping (Electronic Supplementary Material Fig. S4). The nitrous acid heparin treatment such as that used to obtain dalteparin has been previously reported to cause also deamination of some internal glucosamine residues to give by ring contraction a 2-deoxy-2-C-hydroxymethyl pentofuranosidic residues [35–37]. The found chemical shift of the hexocyclic CH₂ group (H2a/b) is in agreement with the value reported previously for methyl-2,5-dideoxy-2-C-(hydroxymethyl)- α -D-xylo-pentofuranoside [36].

Direct LC-MS analysis of RO-LMWHs

To obtain compositional profiles of the RO-LMWHs, their samples were analyzed directly by the LC-MS method in comparison with those of the original unmodified LMWHs. Although a detailed analysis of unmodified LMWHs is outside the scope of this work, some general features of their HPLC-MS chromatograms are described here for comparison with

the corresponding RO-derivatives (Fig. 4 and Fig. S5–S7 of Electronic Supplementary Material).

Oligosaccharides from dp2 up to 22 ($\Delta U_{22,32,0}$, see Electronic Supplementary Material Table S2) were observed in tinzaparin, from dp 2 up to dp 20 ($\Delta U_{20,28,0}$, Fig. 4, see also Electronic Supplementary Material Table S2) in enoxaparin and from dp 4 up to dp 22 ($U_{22,31,0-aM.ol}$ and $U_{22,32,0-aM.ol}$, see Electronic Supplementary Material Table S2) in dalteparin. Comparable results were reported using pentylamine acetate as ion pair reagent for the UPLC separation of tinzaparin oligosaccharides [26] and in an earlier SEC-MS study of Henriksen [33] oligosaccharides up to dp 18 were detected in tinzaparin.

The present LC-MS method highlights both the structural heterogeneity of the analyzed samples and their different molecular weight distributions. For example, while the LC-MS chromatogram of enoxaparin appears highly heterogeneous (Fig. 4), that of dalteparin (Electronic Supplementary Material, Fig. S7), a LMWH known to be extensively purified by ion-exchange chromatography [34], reflects a lower heterogeneity and a lower content of dp4 and dp6 fractions with respect to tinzaparin (Electronic Supplementary Material, Fig. S6) and enoxaparin (Fig. 4, Electronic Supplementary Material Fig. S5). The highly-sulfated even-numbered oligosaccharides are prevalent in all three LMWHs (Electronic Supplementary Material, Fig. S5–S7). *N*-Acetyl groups were observed more frequently within longer chains (Electronic Supplementary Material, Fig. S5–S7).

Peculiar residues typical for each LMWH are clearly observed in their LC-MS profiles. In tinzaparin and enoxaparin LC-MS chromatograms the major components absorb at 232 nm due to the presence of 4,5-unsaturated uronic acids ($\Delta U_{2S}/\Delta U$) at the NRE (Fig. 2) formed as a result of the depolymerisation by β -elimination reaction (LC-UV chromatograms not shown), while analogs bearing saturated uronic acids were found only in low amounts. The enoxaparin LC-MS profile appears more complex due to the presence of oligosaccharides bearing at the RE either hemiacetalic or 1,6-anhydro (1,6aA) forms differing from each other by 18 Da (Fig. 4, Fig. S5). In the LC-MS profile of dalteparin some oligosaccharides containing both aM.ol and Rc residues, detectable due to a mass decrease of 15 Da in comparison with the oligosaccharides bearing only aM.ol residues, have been found (Electronic Supplementary Material, Fig. S7 and Table S2), confirming the ring contracted residues observed in NMR spectra.

Among the minor components, oligosaccharides with an odd number of residues and a glucosamine at the NRE are detectable (Electronic Supplementary Material, Fig. S5–S7) in all three LMWHs, suggesting that some of the original heparin chains terminate with glucosamine units, as previously reported [33,38,39]. Odd-numbered oligosaccharides starting and terminating with uronic acid residues are minor components of tinzaparin (such as $\Delta U_{9,10,1}$, Electronic Supplementary Material Fig. S6 and Table S2) and in dalteparin ($U_{5,6,0}$ and $U_{5,7,0}$, see Electronic Supplementary Material Fig. S7 and Table S2), but are well evident in the enoxaparin ($\Delta U_{5,6,0}$ and $\Delta U_{5,7,0}$, Fig. 4, see also Electronic Supplementary Material, Fig. S5 and Table S2).

Comparison of LC-MS profiles of RO-LMWHs with the corresponding LMWHs (Electronic Supplementary Material Fig S5–S7) provides information on changes in mass values of individual oligosaccharides upon periodate oxidation and borohydride reduction at sites predicted in Fig. 2. A 2 Da mass increase is expected for each internal glycol-split residue with respect to the corresponding unmodified oligosaccharides. The possibility to obtain more structural information by differentiating isomers through RO-modification is also worth noting. For example, after glycol-splitting the enoxaparin tetrasaccharide $\Delta U_{4,5,0}$ gives rise to at least two tetrasaccharides containing internal 2-*O*-sulfated uronic acid

$\Delta U_{4,5,0}$ -ol and a third one containing a nonsulfated uronic acid $\Delta U_{4,5,0,1gs}$ -ol (Electronic Supplementary Material Fig. S5 and Table S2). As particular cases, several gs-ATBR containing oligosaccharides were found (for example, $\Delta U_{8,10,1,2gs}$ -ol and $\Delta U_{10,13,1,2gs}$ -ol, etc, Fig. 4, see also Electronic Supplementary Material Table S2). The possibility to distinguish isomeric oligosaccharides can be shown also for RO-tinzaparin and RO-dalteparin (Electronic Supplementary Material Fig. S6,S7).

LC-MS analysis revealed also the modifications induced by periodate oxidation/sodium borohydrate reduction in the end-groups, confirming the NMR data. The most evident effect of the reduction step is formation of alditol residues at the RE (involving a 2 Da mass increase) for tinzaparin and enoxaparin oligosaccharides originally bearing aminosugars in hemiacetalic form (Fig. 4, Electronic Supplementary Material Fig. S5, S6). The behaviour of some minor short oligosaccharides of enoxaparin such as $\Delta U_{2,3,0}$ and $\Delta U_{3,4,0}$ appearing in RO-enoxaparin as $\Delta U_{2,3,0}$ -ol and $\Delta U_{3,4,0}$ -ol, respectively (Fig. 4), clearly confirms these data. The presence of residues at the RE susceptible to reduction was used for the structural assignment of oligosaccharides in RO-LMWHs: the “first” increment of “2H” was assigned to the reduced RE residue (either glucosamine or uronic acid). A further increase of the mass value of 2 or 4 Da were assigned to oligosaccharides (in the alditol form) with 1 or 2 gs residues, respectively (for example, $\Delta U_{4,5,0,1gs}$ -ol and $\Delta U_{8,10,1,2gs}$ -ol in RO-enoxaparin, Fig. 4). Because the dalteparin RE residues are exclusively constituted by aM.ol (Fig. 2), not susceptible to glycol-splitting nor to borohydrate reduction, the gs-oligosaccharides present in RO-dalteparin are easier to be assigned on the MS basis, because each increment of 2Da should indicate only the presence of one gs-residue.

On the other hand, LC-MS showed that practically all the NRE residues of RO-dalteparin were susceptible to the glycol-splitting and to further chain cleavage (as illustrated in Fig. 5). In the case of the 2-*O*-sulfated uronic acid at the NRE, more represented in dalteparin, the bond between two vicinal OH-groups at C-3 and C-4 can be actually split, while in the case of the nonsulfated uronic acid at the NRE, simultaneous oxidation of the three vicinal OH-groups at C-2, C-3 and C-4 is likely to occur. Further loss of the formed remnants at the NRE (gsI_{2S}(nr) and R(Unr)), respectively, Fig. 5) seems to easily occur. In fact, a relatively large number of RO-dalteparin odd-numbered oligosaccharides start with a glucosamine (see Electronic Supplementary Material Fig. S7). The presence of some remnant-bearing structures was useful for the identification of LMWH oligosaccharides having a saturated uronic acid at the NRE and for distinguishing isomers. For example, the broad U_{8,11,0}-aM.ol peak in the dalteparin LC-MS chromatogram can be explained by the presence of at least two isomers, regular one (constituted by TSD units) and another one having G-A* unit at the NRE that were identified by LC/MS analysis of RO-dalteparin (see Electronic Supplementary Material, Fig S7). The presence of G-A*-bearing oligosaccharides is in agreement with the NMR results showing a relatively high contents of A*, G-(A*) and Gnr residues (see Electronic Supplementary Material Table S1).

Hydrolytic loss of the remnants formed at the NRE were also observed in enoxaparin, which contains low amounts of oligosaccharides starting with glucuronic acid at the NRE (see Electronic Supplementary Material Table S1). For example, R(Unr)-A_{3,5,0}-ol (Fig. 4, see also Electronic Supplementary Material Fig. S5) and R(Unr)-A_{3,5,0-1,6a}A (Electronic Supplementary Material Fig. S5 and Table S2) were observed in RO-enoxaparin and the last one can be structurally correlated with a tetrasaccharide G-A_{NS3S6S}-U_{2S}-A_{NS1.6a}A, isolated from the enoxaparin dp4 fraction (*unpublished data of our group*). A further remnant loss at the NRE is reflected, especially in RO-enoxaparin, by the presence of the trisaccharides A_{3,5,0}-ol and A_{3,6,0}-ol, this latter bearing an A_{NS3S6S} residue.

For species starting with glucosamine at the NRE splitting between C-3 and C-4 is also possible. However, it seems that A5,8,0-1,6aA in enoxaparin (Fig. 4) and A5,8,0-aM.ol in dalteparin (see Electronic Supplementary Material Fig. S7) are resistant to the oxidation because the corresponding analytes were found unchanged in the corresponding RO-derivative chromatograms. Since such components are minor and difficult to characterize, in order to evaluate the susceptibility to glycol-splitting of terminal NRE glucosamine residues the RO-reaction was performed also on a model compound, synthetic pentasaccharide $A_{NS,6S}-G-A_{NS,3S,6S}-I_{2S}-A-OMe_{NS,6S}$ (Arixtra®). This experiment showed that an excess of periodate should be used for completing the splitting of both internal glucuronic acid and glucosamine at the NRE (data not shown). The resistance of the mentioned above oligosaccharides to the periodate oxidation may be also explained by the presence of the 3-*O*-sulfated glucosamine at the NRE of some heparin chains [39]. However, such species may be also formed by the cleavage of the terminal uronic acids, which originally are present in dalteparin and enoxaparin (as described above).

The hypothesis that the formation of the oligosaccharides starting with glucosamine at the NRE as a result of an internal *gs* uronic acids hydrolysis could not be confirmed because no corresponding remnant (R, Fig. 1e) bearing oligosaccharides were found. However, to verify if the developed LC-MS method permits to detect such species a RO-tinzaparin sample was prepared using HCl instead of acetic acid, for neutralizing the $NaBH_4$ -reaction mixture. The NMR spectrum of the HCl treated preparation (not shown) showed a lower amount of generated *gs* residues than in the preparation treated with acetic acid, supporting the hypothesis that partial hydrolysis occurred. Indeed, a number of remnant (R) bearing species was observed (Electronic Supplementary Material Fig. S6), indicating that the present analytical conditions permit to observe and monitor such a hydrolysis process.

Elution order

For oligosaccharides with the same dp, the higher the sulfation degree, the higher the retention time RT (for example, $RT(\Delta U_{6,7,0}) < RT(\Delta U_{6,8,0}) < RT(\Delta U_{6,9,0})$ in enoxaparin Fig. 4). The presence of a *N*-acetyl group causes a slight increase of the retention time ($RT(\Delta U_{6,7,0}) < RT(\Delta U_{6,7,1})$) that indicates that not only electrostatic but also hydrophobic interactions between analytes and stationary phase can take place. Unexpectedly, the retention time of $\Delta U_{16,21,0}$ is somewhat lower than that of $\Delta U_{14,21,0}$ in tinzaparin (Electronic Supplementary Material Fig. S6) and enoxaparin (Electronic Supplementary Material Fig. S5). This finding may be explained by the fact that the longer the oligosaccharide chains, the less the influence of additional disaccharide units and the more crucial the influence of the number of anionic groups per chain. Enoxaparin oligosaccharides with a 1,6aA-residues are eluted after their analogues bearing hemiacetalic aminosugars ($RT(\Delta U_{6,8,0}) < RT(\Delta U_{6,8,0-1,6aA})$). Unsaturation in the NRE uronic acid increases the RT ($RT(U_{6,9,0}) < RT(\Delta U_{6,9,0})$), probably due to the higher acidity of the uronic acid carboxy-group when conjugated with a double bond, leading to a stronger interaction with dibutylammonium cation. The same fact may take place in the case of the odd enoxaparin oligosaccharides starting with $\Delta U_{(2S)}$, which shows higher RT than oligosaccharides starting with a glucosamine residue ($RT(A_{3,4,0}) < RT(\Delta U_{3,4,0})$); moreover, $\Delta U_{3,4,0}$, bearing two carboxyl groups, have more anion centres able to interact with dibutylammonium cation. Oligosaccharides in alditol form are eluted after their unmodified analogs ($RT(\Delta U_{6,8,0}) < RT(\Delta U_{6,8,0-ol})$), and this is probably caused by the higher flexibility of the reduced open form with respect to that of the hemiacetalic one that facilitates the interactions between sulfate groups and dibutylamine on the stationary phase. The presence of an uronic acid remnant increases the retention time (e.g., in RO-tinzaparin ($RT(\Delta U_{8,12,0-ol}) < RT(\Delta U_{8,12,0-R})$), probably, due to the additional charge of the remnant carboxyl group (R) present at the RE (Fig. 1e).

LC-MS profiling of heparinase-digested RO-LMWHs

The main limitation in LC-MS profiling of LMWHs and their RO-derivatives is that only the major species can be separated and identified; in fact, component overlapping in terms of retention times and mass values, makes difficult to characterize the minor components. This problem becomes more crucial for higher oligosaccharides, especially when unmodified oligosaccharides and glycol-split ones have similar retention times. The gradient optimization for LMWHs is limited by the total analysis time due to the wide range of the species to be profiled, from dp 2 up to at least dp 22.

In order to obtain more informative data, all RO-LMWHs were also analyzed after exhaustive enzymatic digestion with a mixture of heparinases I, II and III which leads to concentration of sequences containing gs-residues and to the identification of peculiar structures otherwise difficult to be characterized. The LC-MS profiles of heparinase-digested RO-LMWHs (Fig. 6, and v Fig. S8, S9) are definitely simpler than those of the corresponding non-digested samples (Fig. 4, Fig. S5–S7). Like those of similarly digested RO-heparins [13], they essentially consist of disaccharide, tetrasaccharide, hexasaccharide fragments and very low amounts of some octasaccharides present only in the digest of RO-dalteparin (see Electronic Supplementary Material Fig. S9). The major disaccharide $\Delta U_{2,3,0}$ ($\Delta U_{2S-A_{NS6S}}$), the minor disaccharide $\Delta U_{2,2,0}$ ($\Delta U_{2S-A_{NS}}$) and several tetrasaccharides resistant to the enzymatic cleavage (such as, $\Delta U_{4,6,0-ol}$ in RO-tinzaparin, $\Delta U_{4,5,0-1,6aA}$ in RO-enoxaparin, $\Delta U_{4,5,0-aM.ol}$ in RO-dalteparin) are also present in the corresponding digest of LMWHs (not shown), characterizing the regular sequences not containing nonsulfated uronic acids.

The fragments derived from enzymatic digestion of RO-LMWHs differ from those of unmodified LMWHs especially in their hexasaccharide components, which are practically absent in the heparinase digests of non-gs LMWHs (not shown). It is important to note that while the species containing two gs residues are seldom observable in the profiles of the intact RO-LMWHs (Fig. 4 and Electronic Supplementary Material Fig. S5–S7), some of these species can be detected in the chromatograms of all the RO-LMWHs digests (for example, $\Delta U_{6,7,1,2gs}$, Fig. 6).

As expected, the digested RO-tinzaparin also consists of even-numbered oligosaccharides terminating at the RE with both hexosamine formed during the enzymatic cleavage and some with alditols generated by the RO-reaction (see Electronic Supplementary Material Fig. S8). Notably, no disaccharide in alditol form was detected (see Discussion).

The LC-MS profile of RO-enoxaparin enzymatic digest (Fig. 6), is definitely more complex, especially as regards end residues, than the corresponding profiles of RO-tinzaparin and RO-dalteparin digests, making structural assignments more difficult. Since nonsulfated uronic acids of RO-LMWH chains are split and cannot be recognized by the heparinases, the 4,5-unsaturated uronic acid residues were assumed to be always 2-*O*-sulfated for the oligosaccharides present in the RO-LMWH digests. Furthermore, to verify if the observed mass increment of 2 Da was caused by the generation of one internal gs residue or by reduction of terminal hemiacetal, the RO-enoxaparin digest was further treated with sodium borohydride (profiles not shown). Species susceptible to this reduction (i.e., those converted to alditol forms) are identified with oligosaccharides originally terminating with reducing hexosamines and consequently bearing internal gs, while the reduction resistant oligosaccharides were considered to already have an alditol group at the RE. This approach was used to distinguish $\Delta U_{4,6,0-ol}$ (Fig. 6) and $\Delta U_{4,6,0,1gs}$ (not shown in the chromatogram); this minor tetrasaccharide, contains a *N*-sulfated-glucosamine-3,6-*O*-disulfate residue and is likely to be one of the markers of the sulfated ATBR ($I_{2S-A_{NS6S}}-G-$

$A_{NS3S6S-I2S-A_{NS6S}}$), previously observed in the enzymatic digest of RO-heparin from bovine lung [13].

The LC-MS chromatogram of the heparinase-digest of RO-dalteparin (see Electronic Supplementary Material Fig. S9) is less complex than those of the other two RO-LMWH digests, reflecting in part a rather homogeneous internal structure of the original LMWH and the fact that practically all chains in the original dalteparin terminate at the RE with aM.ol groups, resistant to the glycol-splitting. Notably, the RO-dalteparin digests contain also octasaccharides $\Delta U_{8,9,1,1gs-aM.ol}$ and $\Delta U_{8,9,1,2gs-aM.ol}$ (both in traces), indicating that all the glycosidic bonds of these oligosaccharides are resistant to cleavage by heparinases (see Discussion).

RO-induced modifications of peculiar end-groups (linkage region, mannosamine, 1,6-anhydromannosamine)

The LC-MS chromatogram of tinzaparin reveals the presence of species containing intact linkage region such as $\Delta U_{4,3,1-LR}$, $\Delta U_{4,4,1-LR}$, $\Delta U_{8,6,2-LR}$, $\Delta U_{8,9,1-LR}$, $\Delta U_{10,11,1-LR}$ and $\Delta U_{10,11,2-LR}$ (see Electronic Supplementary Material Fig. S6).

As expected and illustrated in Fig. 1, the glucuronic acid and xylose units of the LR are susceptible to glycol-splitting, and, depending on the reaction conditions the LR can generate two forms, such as the one shown in Fig. 1d (gsLR) or further hydrolyzed at the level of gs-xylose, to give the serine lacking fragment $gsG-Gal-Gal-CH(CH_2OH)_2$ (gsLR(2)).

The LC-MS analysis of the oligosaccharides containing the gsLR/gsLR(2) in the RO-tinzaparin digest allowed the characterization of the environment near the LR. Of note, $\Delta U_{2,1,1-gsLR(2)}$ is formed in trace amount, which indicates that the first uronic acid preceding G_{LR} is almost always nonsulfated. Different tetrasaccharides containing one gs residue linked to the gsLR(2), such as $\Delta U_{4,3,1,1gs-gsLR(2)}$, $\Delta U_{4,4,1,1gs-gsLR(2)}$ and $\Delta U_{4,2,1,1gs-gsLR(2)}$, were detected. The first level structure of the former corresponds to the previously observed heparin oligosaccharides $\Delta U_{2S-A_{NS6S}-G/I-A_{NAc}-LR}$ [23]. Only one specie containing two acetyl groups ($\Delta U_{4,1,2,1gs-gsLR(2)}$) was observed, but in very low amounts, indicating that, when the second uronic acid after G_{LR} is 2-*O*-sulfated, the second glucosamine residue is almost always *N*-sulfated and not *N*-acetylated. Moreover, the presence of $\Delta U_{4,4,1,1gs-gsLR(2)}$ indicates that the first *N*-acetylglucosamine can also be 6-*O*-sulfated, as also found in heparin [23]. Among higher oligosaccharides, $\Delta U_{6,3,2,2gs-gsLR(2)}$ and $\Delta U_{6,2,2,2gs-gsLR(2)}$ were the most evident, while a mono-*N*-acetylated analog ($\Delta U_{6,3,1,2gs-gsLR(2)}$) was observed in trace. Notably, no species with three *N*-acetylglucosamines were found. Considering the known biosynthesis pathway of heparin [40], these data could indicate that when the second uronic acid after G_{LR} is nonsulfated, the following glucosamine is *N*-acetylated. Octasaccharide chains with three gs units linked to the gsLR(2) were also found, even if in traces (Electronic Supplementary Material Table S2). Combining these data with the results obtained by the LC-MS analysis of the intact RO-tinzaparin, it is likely that the *N*-acetylated domain in the closest proximity of LR of the parent heparin should be very short (i.e., di- or tetrasaccharide sequences).

Several gsLR-bearing oligosaccharides with the sulfation/acetylation pattern similar to that observed in tinzaparin were found also in enoxaparin after SEC-fractionating its digested RO-derivative (Electronic Supplementary Material Fig. S10). No oligosaccharides bearing 2-*O*-phosphorylated xylose [41] were observed. It would probably be possible to detect these particular LR-bearing oligosaccharides after previous isolation of the LR-containing fraction.

In the LC-MS chromatogram of the digested RO-enoxaparin, an oligosaccharide with m/z 507.476⁽²⁻⁾ attributed to a Δ U3,5,0- aminosugar remnant (Δ U3,5,0-Ram) structure was observed (neutral molecular formula $C_{22}H_{35}N_1O_{34}S_5$, theoretical m/z 507.475) (Fig. 5,6). The formation of this trisaccharide, also found in RO-tinzaparin and some RO-heparins [13], as a trace component, may be explained by the oxidation of glucosamines bearing free NH_2 -groups, which can be present in heparin. The same explanation does not hold for RO-enoxaparin, where Δ U3,5,0-Ram is present in relatively high quantity. Notably, 2D NMR spectrum of the parent enoxaparin did not show cross peaks of glucosamines with free NH_2 . We suggest that the generation of Δ U3,5,0-Ram in RO-enoxaparin could result from an oxidation of the *N*-sulfated mannosamine residue (Fig. 5,6).

Other unknown structures were observed (m/z 448.5, 449.5 and 488.5) in the heparinase-digest of RO-enoxaparin. The LC-MS data show that these analytes are likely to have the same backbone but differ by number of sulfate-, acetyl groups, and gs residues (Electronic Supplementary Material Table S3). The fact that all the three species absorb at 232 nm indicates the presence of an unsaturated uronic acid at the NRE. Useful information was obtained especially by a subsequent SEC-fractionation. LC-MS analysis showed that the SEC-fraction eluted between tri- and tetrasaccharides pools is enriched in compounds of the unknown structures (m/z 448.5, 449.5 and 488.5, see Electronic Supplementary Material Fig. S10), that is in agreement with the hypothesized neutral formula (with an error less than 5 ppm) (see Electronic Supplementary Material Table S3). These species were also found to be resistant to borohydride reduction, suggesting that they do not have hemiacetalic monosaccharide at the RE.

Two different structures with the same neutral formula were found to correspond to the observed unusual m/z values: the first one with the same backbone as Δ U3,5,0-Ram but containing *N*-acetylated glucosamine, and the second structure bearing a split 1,6-anhydro-aminosugar at the RE (gs1,6a, Fig. 5 and Electronic Supplementary Material Table S4). A subsequent MS/MS experiment indicated that the main observed fragments could be formed from both backbone types (either an acetylated trisaccharide with an aminosugar remnant, or a tetrasaccharide with gs1,6a) (see Electronic Supplementary Material Fig. S11). Several minor signals may be more informative. For example, m/z 247,494 may correspond to a disaccharide unit with two sulfate groups, suggesting that the only glucosamine is sulfated but not acetylated, ruling out the structure with a remnant and a *N*-acetyl substituent.

Moreover, the HSQC spectrum of the SEC fraction enriched in structurally unknown compounds did not show cross-peaks corresponding to the *N*-acetyl-glucosamine-6-*O*-sulfate linked to 2-*O*-sulfated-iduronic acid ($A_{NAC6S-I2S}$) C1-H 5.15/96.6 ppm, C2-H 4.03/56.2 ppm [42]. This cross-peak should have been observed if the unknown compound with m/z 488.5 had the acetylated structure Δ U_{2S}- $A_{NAC6S-I2S}$ -Ram. Notably, the $A_{NAC6S-I2S}$ unit is rarely present within heparin chains. Therefore, all experimental data, i.e.: i) absorbance at 232 nm; ii) resistance under the reductive conditions; iii) accurate m/z value; iv) correspondence of the experimental isotopic pattern with theoretic one; v) resistance to the reduction and to the enzymatic cleavage; and vi) NMR data, confirm that the structure with the split 1,6-anhydromannosamine is the most probable.

Sequences with three subsequent glycol-split residues

The sequences with three glycol-split uronic acids in contiguous disaccharide units were previously observed in trace amounts in the heparinase-digest of the RO-derivative of pig mucosal heparin [13]. This indicates that sequences with three subsequent nonsulfated uronic acid units are present within heparin chains. A similar result was obtained for the RO-tinzaparin where octasaccharides with three internal gs units and glycol-split LR sequence were found (described above). A fraction containing highly sulfated mono-*N*-

acetylated octasaccharides with three gs units ($\Delta U_{8,7,1,3gs}$, $\Delta U_{8,8,1,3gs}$, $\Delta U_{8,9,1,3gs}$) was isolated from the RO-enoxaparin digest by SEC fractionation (see Electronic Supplementary Material Fig. S10). Borohydride reduction revealed that octasaccharides with both three gs-units ($\Delta U_{8,7,1,3gs}$, $\Delta U_{8,8,1,3gs}$, $\Delta U_{8,9,1,3gs}$) and two gs-units and reduced aminosugar at the RE ($\Delta U_{8,7,1,2gs-ol}$, $\Delta U_{8,8,1,2gs-ol}$, $\Delta U_{8,9,1,2gs-ol}$, $\Delta U_{8,10,1,2gs-ol}$) were present. The cross-peak of the α -*N*-sulfated glucosamine ($A_{NS\alpha}$), observed in the 2D NMR spectrum of the digest before reductive treatment, confirms the presence of octasaccharides with three gs units and hemiacetalic *N*-sulfated glucosamine at the RE. It is worth noting that in the case of the octasaccharides with two gs residues their resistance to the enzymatic cleavage may be explained by the position of the 2-*O*-sulfated uronic acid (U_S) that is likely to be close to the alditol unit in the proposed structure $\Delta U_S\text{-A-gsU-A-gsU-A-U}_S\text{-A-ol}$.

Discussion

Modifications generated in LMWHs by the glycol-splitting periodate oxidation followed by a “stabilizing” borohydride reaction mainly involve internal nonsulfated uronic acid residues and end-residues susceptible to splitting and/or reduction. These structural modifications change both NMR spectra and LC-MS profiles of the LMWHs, providing complementary and characteristic fingerprints of both LMWHs and their RO-derivatives. Thus, the combined NMR/LC-MS analysis can allow to characterize the individual RO-LMWH, compare different RO-samples and provide structural information on the starting material. Whereas the HSQC spectra are currently exploited for quantitative evaluation of individual monosaccharide and disaccharide units in heparins [32] and LMWHs [2], a note of caution is necessary when dealing with gs-derivatives, since the local flexibility of gs residues may affect their relaxation times and scalar coupling values. The reported quantitative data (Online Resource 3), though compatible with our overall conclusions, should accordingly be taken as provisional, until a deeper study is made using well-defined model compounds.

The HSQC NMR spectra and the LC-MS profiles of RO-LMWHs also retain some features characteristic of the LMWH production method, partial depolymerisation with heparinase I (tinzaparin), base-catalyzed β -elimination (enoxaparin), and nitrous acid depolymerisation (dalteparin). All of these depolymerisation methods cleave only glycosidic bonds between an aminosugar and the adjacent uronic acid that leads to the formation of even-numbered oligosaccharides (Fig. 2). Surprisingly, RO-dalteparin has been shown to contain numerous odd-numbered oligosaccharides (see Electronic Supplementary Material Fig. S7), probably due to the glycol-splitting of the dalteparin terminal uronic acid residues bearing 3,4-diol groups and the further hydrolysis of the generated remnants (Fig. 5). Together with the observed high content of odd-numbered oligosaccharides, the occurrence of occasional ring contracted residues diversifies RO-dalteparin from the other RO-LMWHs.

Interestingly, RO-enoxaparin was the only one, among the RO-LMWHs of the present study, showing a LC-MS profile less complex than that of the parent LMWH (Fig. 4). This can be reasonably explained by the presence of end residues ΔU_{2S} at the NRE, and *N*-sulfated 1,6aA groups at the RE, resistant to glycol-splitting. Minor ΔU residues from one side, as well as the above mentioned 1,6aM on the other side, may both contribute to some chain shortening caused by their oxidation. While, the glycol-splitting of the ΔU was expected, the oxidation of the *N*-sulfated 1,6aM residues not bearing two vicinal hydroxyls was quite unexpected.

Hydrolytic cleavage of glycosidic bonds (especially those of the gsU-residues), as well as partial cleavage and eventual hydrolysis at the level of terminal gs residues should be considered as possible events under the chosen conditions of RO-reaction. For example, addition of both sodium borohydride and strong acids (for example, hydrochloric acid) used

for the pH adjustment, may represent critical steps since it can locally generate high basic or acidic conditions [12,13]. We observed that the acidic hydrolytic effect can be decreased by using mild acids (i.e. acetic acid). Although under our experimental conditions the conversion yields of the parent LMWHs to the corresponding RO-derivatives are quite high (>85%), the decrease (~20%) observed in their average MW (see Experimental) indicates some chain shortening with respect the parent LMWHs. Remnant bearing species, markers of such a chain cleavage, can be detected by the developed LC-MS method.

The plurality of species observed in the LC-MS chromatograms of RO-LMWHs suggests that some minor components may result from side-reactions such as hydrolysis at the level of internal gs residues (with generation of shorter chains terminating with remnant residues), oxidation of some end groups, and/or further cleavage of the generated remnants. In view of a further optimization of the RO-reaction conditions that could limit the impact of side-reactions, the present LC-MS method represents an useful and reproducible tool for fingerprinting RO-LMWH.

On the other hand, the glycol-splitting-induced local mobility is likely to exert an influence on retention times in LC-MS profiles of components of RO-LMWHs, allowing separation of some isomeric oligosaccharides otherwise difficult to achieve.

LC-MS analysis of heparinase digests provide additional structural information on oligosaccharide components of RO-LMWHs, and, indirectly, on the parent compounds. Since heparin lyases recognize the “regular” sequences of heparin but not residues introduced by the depolymerisation reactions [24,43,44] nor glycol-split residues [13], incubation of RO-LMWHs with heparinases generated fragments one or more disaccharide unit(s) longer than the corresponding ones detected in the LMWH digests, with incorporated gs-units, providing information about the length of the undersulfated heparin sequences. The combination of glycol-splitting and enzymatic digestion demonstrated that the sequences containing up to three subsequent nonsulfated uronic acids are present within heparin chains.

The specificity of the heparinases can be exploited for confirming the structure of terminal residues at the RE (such as 1,6aA in RO-enoxaparin and aM.ol in RO-dalteparin) and some sequences bearing them. As implied in previous reports on enoxaparin and dalteparin in different contexts [24,43,44], these residues at the RE are not recognized by heparinases and tetrasaccharide fragments are generated instead of disaccharides as would be the case if the end residues were unmodified glucosamines. The present study suggests that also the terminal alditols (as observed for practically all species of RO-tinzaparin, and for a number of chains in RO-enoxaparin) exert some inhibition of heparinases, with preferential cleavage of glycosidic bonds one disaccharide unit further towards the NRE. In fact, LC-MS peaks attributable to alditol disaccharides were never observed in the enzymatic digests, indicating that the heparinase-generated RO-LMWH fragment terminating with an alditol cannot be shorter than a trisaccharide (for example, $\Delta U3,4,0\text{-ol}$).

An additional inhibition exerted by glycol-split residues, first observed by us on RO-derivatives of full-length heparins [13], permitted to characterize the heparin sequences near the linkage region by the first time, and to identify the ATBR-containing sequences with different sulfation/acetylation pattern. These ATBR-derived fragments can be more easily unraveled because the glycosidic bond of 3-O-sulfated glucosamine (A*) is preferentially cleaved by heparinases and the A*-containing oligosaccharides terminate with a “truncated” N,3,6-trisulfated glucosamine [45]. The ATBR-derived fragments accordingly terminate at the RE with a G-A* disaccharide; moreover, since both the bond connecting glucosamine to the gsG-A* unit [46] and that of the gs-residue (gsI) linked to the next sequence (A-gsG-A*) [13] are not cleaved by heparinases, most of these typical fragments have the minimum size

of a hexasaccharide. The hexasaccharide $\Delta U_{6,7,1,2gs}$ (in the case of dalteparin it could be also incorporated in the minor octasaccharide $\Delta U_{8,9,1,2gs-aM.ol}$) was observed in the LC-MS profiles of all the RO-LMWH digests. Tetrasaccharide $\Delta U_{4,6,0,1gs}$ (generated from the highly sulfated ATBR variant [13]) was also found in trace amount in all RO-LMWHs digests.

Conclusions

This work provides previously unavailable criteria for structural analysis of gs-LMWHs as well as a complement to current methods for characterization of LMWHs. In particular, combined 2D NMR and LC-MS analysis permits the detection of the major internal modifications introduced in LMWH chains by periodate oxidation/borohydride reduction. Modifications of end residues susceptible to glycol-splitting and /or reduction can also be detected by this approach. In addition, the present analysis of RO-LMWHs and their heparinase digests provides an informative profiling complementary to that currently obtained for unmodified LMWHs, and a better characterization of isomeric oligosaccharides. The combination of glycol-splitting and enzymatic digestion provides more informative data also on the starting material, first of all, about the length of the sequences containing subsequent nonsulfated uronic acids and the structure of terminal sequences in RO-LMWHs. In particular, the *N*-acetylated domain in the closest proximity to the LR was characterized using this approach, providing information on the heparin biosynthesis. ATBR-containing oligosaccharides can be identified by the LC-MS analysis of RO-LMWHs and their heparinase-digests. Additionally, the NMR/LC-MS approach permits monitoring of the efficiency of conversion of nonsulfated uronic acids to the corresponding gs residues as well as the extent of side reactions occurring under different experimental conditions such as cleavage of remnants of terminal gs residues and hydrolysis of internal ones.

Supplementary Material

Refer to Web version on PubMed Central for supplementary material.

Acknowledgments

This work was supported by the National Institute of Health (grant number R01-CA138535) and The Italian Association for Cancer Research (AIRC, grant number IG10569).

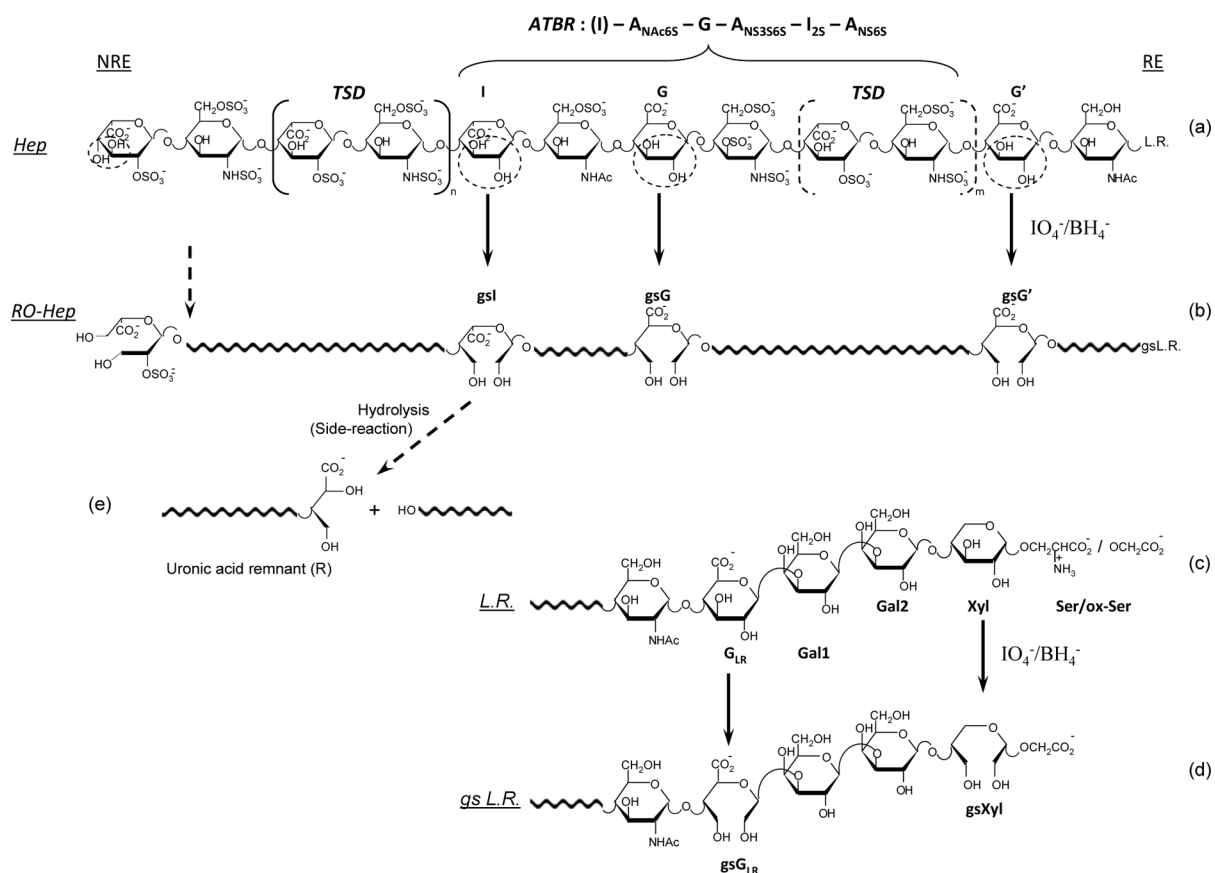
References

1. Weitz JI. Low-molecular weight heparins. *N Engl J Med*. 1997; 337:688–698. [PubMed: 9278467]
2. Guerrini M, Guglieri S, Naggi A, Sasisekharan R, Torri G. Low molecular weight heparins: structural differentiation by bidimensional nuclear magnetic resonance spectroscopy. *Semin Thromb Hemost*. 2007; 33:478–487. and references therein. [PubMed: 17629844]
3. Casu, B. *Chemistry and Biology of Heparin and Heparan Sulfate*. Garg, HG.; Linhardt, RJ.; Hales, CA., editors. Elsevier; Amsterdam: 2005. and references therein
4. Lever R, Page CP. Novel drug development opportunities for heparin. *Nat Rev Drug Discov*. 2002; 1:140–148. [PubMed: 12120095]
5. Fuster MM, Esko JD. The sweet and sour of cancer: glycans as novel therapeutic agents. *Nat Rev Cancer*. 2005; 5:526–542. [PubMed: 16069816]
6. Casu B, Vlodavsky I, Sanderson RD. Non-anticoagulant heparins and inhibition of cancer. *Pathophysiol Haemost Thromb*. 2007; 36:195–203. [PubMed: 19176992]
7. Casu B, Naggi A, Torri G. Heparin-derived heparan sulfate mimics to modulate heparan sulfate-protein interaction in inflammation and cancer. *Matrix Biology*. 2010; 29:442–452. and references therein. [PubMed: 20416374]

8. Höök M, Björk I, Hopwood J, Lindahl U. Anticoagulant activity of heparin: separation of high-activity and low-activity heparin species by affinity chromatography on immobilized antithrombin. *FEBS Lett.* 1976; 66:90–93. [PubMed: 1278445]
9. Naggi, A. *Chemistry and Biology of Heparin and Heparan Sulfate*. Garg, HG.; Linhardt, RJ.; Hales, CA., editors. Elsevier; Amsterdam: 2005. and references therein
10. Mousa SA, Linhardt R, Francis JL, Amirkhosravi A. Anti-metastatic effect of a non-anticoagulant low-molecular-weight heparin versus the standard low-molecular-weight heparin, enoxaparin. *Thromb Haemost.* 2006; 96:816–821. [PubMed: 17139378]
11. Perlin AS. Glycol-cleavage oxidation. *Advances Carbohydr Chem Biochem.* 2008; 60:183–250. [PubMed: 16750444]
12. Islam T, Butler M, Sikkander SA, Toida T, Linhardt RJ. Further evidence that periodate cleavage of heparin occurs primarily through the antithrombin binding site. *Carbohydr Res.* 2002; 337:2239–2243. [PubMed: 12433488]
13. Aleksseva A, Casu B, Torri G, Pierro S, Naggi A. Profiling glycol-split heparins by high-performance liquid chromatography/mass spectrometric analysis of their heparinase-generated oligosaccharides. *Anal Biochem.* 2013; 434:112–122. [PubMed: 23201389]
14. Casu B, Guerrini M, Naggi A, Perez M, Torri G, Ribatti D, Carminati P, Giannini G, Penco S, Pisano C, Belleri M, Resnati M, Presta M. Short heparin sequences spaced by glycol-split uronate residues are antagonists of fibroblast growth factor 2 and angiogenesis inhibitors. *Biochemistry.* 2002; 41:10519–10528. [PubMed: 12173939]
15. Naggi A, Casu B, Perez M, Torri G, Cassinelli G, Penco S, Pisano C, Giannini G, Ishai-Michaeli R, Vlodavsky I. Modulation of the heparanase-inhibiting activity of heparin through selective desulfation, graded N-acetylation, and glycol-splitting. *J Biol Chem.* 2005; 280:12103–12113. [PubMed: 15647251]
16. Hostetter N, Naggi A, Torri G, Ishai-Michaeli R, Casu B, Vlodavsky I, Borsig L. P-selectin and heparanase-dependent antimetastatic activity of non-anticoagulant heparins. *FASEB J.* 2007; 21:3562–3572. [PubMed: 17557930]
17. Leitgeb AM, Blomqvist K, Cho-Ngwa F, Samje M, Nde P, Titanji V, Wahlgren M. Low anticoagulant heparin disrupts *Plasmodium falciparum* rosettes in fresh clinical isolates. *Am J Trop Med Hyg.* 2011; 84:390–396. [PubMed: 21363975]
18. Ekman-Ordeberg G, Hellgren M, Åkerud A, Andersson E, Dubicke A, Sennström M, Byström B, Tzortzatos G, Gomez MF, Edlund I, Lindahl U, Malmström. A Low molecular weight heparin stimulates myometrial contractility and cervical remodeling in vitro. *Acta Obstetr et Gynecol Scand.* 2009; 88:984–989.
19. Vogt AM, Pettersson F, Moll K, Johnsson C, Normark J, Ribacke U, Egwang TG, Ekre H-P, Spilmann D, Chen Q, Wahlgren M. Release of sequestered malaria parasites upon injection of a glycosaminoglycan. *PLoS Pathogens.* 2006; 2:0853–0863.
20. Weitz JI, Young E, Johnston M, Stafford AR, Fredenburgh JC, Hirsh J. Vasoflux, a new anticoagulant with a novel mechanism of action circulation. *Circulation.* 1999; 99:682–689. [PubMed: 9950667]
21. Zhou H, Roy S, Cochran E, Zouaoui R, Chu CL, Duffner J, Zhao G, Smith S, Galcheva-Gargova Z, Karlgren J, Dussault N, Kwan RYQ, Moy E, Barnes M, Long A, Hohann C, Qi YW, Shriver Z, Ganguly T, Schultes B, Venkataraman G, Kishimoto TK. M402, a novel heparan sulfate mimetic, targets multiple pathways in tumor progression and metastasis. *PLoS ONE.* 2011; 6:e21106.10.1371/journal.pone.0021106
22. Xiao Z, Tappen BR, Ly M, Zhao W, Canova LP, Guan H, Linhardt RJ. Heparin mapping using heparin lyases and the generation of a novel low molecular weight heparin. *J Med Chem.* 2011; 54:603–610. [PubMed: 21166465]
23. Iacomini M, Casu B, Guerrini M, Naggi A, Pirola A, Torri G. “Linkage region” sequence of heparin and heparan sulfate: Detection and quantification by Nuclear Magnetic Resonance spectroscopy. *Anal Biochem.* 1999; 274:50–58. and references therein. [PubMed: 10527496]
24. Linhardt RJ, Loganathan D, Al-Hakim A, Wang H-M, Walenga JM, Hoppensteadt D, Fareed J. Oligosaccharide mapping of low-molecular weight heparins: structure and activity differences. *J Med Chem.* 1990; 33:1639–1645. [PubMed: 2160537]

25. Capila, I.; Gunay, NS.; Shriver, Z.; Venkataraman, G. *Chemistry and Biology of Heparin and Heparan Sulfate*. Garg, HG.; Linhardt, RJ.; Hales, CA., editors. Elsevier; Amsterdam: 2005.
26. Langeslay DJ, Urso E, Gardini C, Naggi A, Torri G, Larive CK. Reversed-phase ion-pair ultra-high-performance-liquid chromatography-mass spectrometry for fingerprinting low-molecular-weight heparins. *J Chromatogr A*. 2013; 1292:201–210. [PubMed: 23352830]
27. Korir AK, Limtiaco JF, Gutierrez SM, Larive CK. Ultrapformance ion-pair liquid chromatography coupled with electrospray time-of flight mass spectrometry for compositional profiling and quantification of heparin and heparan sulphate. *Anal Chem*. 2008; 80:1297–1306. [PubMed: 18215021]
28. Kuberan B, Lech M, Zhang L, Wu LZ, Beeler DL, Rosenberg R. Analysis of heparan sulfate oligosaccharides with ion pair-reverse phase capillary high performance liquid chromatography-microelectrospray ionization time-of-flight mass spectrometry. *J Am Chem Soc*. 2002; 124:8707–8718. [PubMed: 12121115]
29. Doneanu CE, Chen W, Geber JC. Analysis of oligosaccharides derived from heparin by ion-pair reverse-phase chromatography/mass spectrometry. *Anal Chem*. 2009; 81:3485–3499. [PubMed: 19344114]
30. Wang B, Buhse LF, Al-Hakim A, Boyne MT II, Keire DA. Characterization of currently marketed heparin products: analysis of heparin digests by RPIP-UHPLC-QTOF-MS. *J Pharm Biomed Anal*. 2012; 67–68:42–50.
31. Vann WF, Schmidt MA, Jann B, Jann K. The Structure of the Capsular Polysaccharide (K5 Antigenn) of Urinary-Tract-Infective *Escherichia coli* 010:K5:H4. *Eur J Biochem*. 1981; 116:359–364. [PubMed: 7018909]
32. Guerrini M, Naggi A, Guglieri S, Santarsiero R, Torri G. Complex glycosaminoglycans: profiling substitution patterns by two-dimensional nuclear magnetic resonance spectroscopy. *Anal Biochem*. 2005; 337:35–47. [PubMed: 15649373]
33. Henriksen J, Ringborg LH, Roepstorff P. On-line size-exclusion chromatography/mass spectrometry of low molecular mass heparin. *J Mass Spec*. 2004; 39:1305–1312.
34. Bisio A, Vecchietti D, Citterio L, Guerrini M, Raman R, Bertini S, Eisele G, Naggi A, Sasisekharan R. Structural features of low-molecular weight heparins affecting their affinity to antithrombin. *Thromb Haemost*. 2009; 102:865–873. [PubMed: 19888521]
35. Shively JE, Conrad HE. Stoichiometry of the Nitrous Acid Deaminative Cleavage of Model Amino Sugar Glycosides and Glycosaminoglycuronans. *Biochem*. 1970; 9:33–43. [PubMed: 4243761]
36. Baer HH, Astles DJ, Chin H-C, Siemsen L. The formation of branched-chain deoxypentofuranosides by ring contraction in the reductive desulfonyloxylation of hexopyranoside p-toluenesulfonates. *Can J Chem*. 1985; 63:432–439.
37. Horton D, Philips KD. The nitrous acid deamination of glycosides and acetates of 2-amino-2-deoxy-D-glucose. *Carbohyd Res*. 1973; 30:367–374.
38. Thanawiroon C, Rice KG, Toida T, Linhardt RJ. Liquid chromatography/mass spectrometry sequencing approach for highly sulfated heparin-derived oligosaccharides. *J Biol Chem*. 2004; 279:2608–2615. [PubMed: 14610083]
39. Rudd TR, Macchi E, Muzi L, Ferro M, Gaudesi D, Torri G, Casu B, Guerrini M, Yates EA. Unravelling structural information from complex mixtures utilising correlation spectroscopy applied to HSQC spectra. *Anal Chem*. 2013; 1021/ac4014379
40. Lindahl U, Feingold DS, Roden L. Biosynthesis of heparin. *Trends Biochem Sci*. 1986; 11:221–225.
41. Tone Y, Pedersen LC, Yamamoto T, Izumikawa T, Kitagawa H, Nishihara J, Tamura J, Negishi M, Sugahara K. 2-O-Phosphorylation of xylose and 6-O-sulfation of galactose in the protein linkage region of glucosaminoglycans influence the glucuronyltransferase-I activity involved in the linkage region synthesis. *JBC*. 2008; 283:16801–16807.
42. Yates EA, Santini F, Guerrini M, Naggi A, Torri G, Casu B. 1H and 13C NMR spectral assignments of the major sequences of twelve systematically modified heparin derivatives. *Carbohydr Res*. 1996; 294:15–27. [PubMed: 8962483]
43. Viskov, C.; Mourier, P. Method for quantitatively determining specific groups constituting heparins of low molecular weight heparins. *US Pat Appl US 2004/0265943 A1*. 2004.

44. Ozug J, Wudyka S, Gunay NS, Beccati D, Lansing J, Wang J, Capila I, Shriver Z, Kaundinya GV. Structural elucidation of the tetrasaccharide pool in enoxaparin sodium. *Anal Bioanal Chem.* 2012; 403:2733–2744. [PubMed: 22610547]
45. Xiao Z, Zhao W, Yang B, Zhang Z, Guan H, Linhardt RJ. Heparinase 1 selectivity for the 3,6-di-*O*-sulfo-2-deoxy-2-sulfamido- α -*D*-glucopyranose (1,4) 2-*O*-sulfo- α -*L*-idopyranosyluronic acid (GlcNS3S6S-IdoA2S) linkages. *Glycobiol.* 2011; 21:13–22.
46. Shriver Z, Sundaram M, Venkataraman G, Fareed J, Linhardt R, Biemann K, Sasisekharan R. Cleavage of the antithrombin III binding site by heparinases and its implication in the generation of low-molecular weight heparin. *Proc Natl Acad Sci USA.* 2000; 97:10365–10370. [PubMed: 10984532]

**Fig. 1.**

Simplified formula of a representative ATBR-containing chain of porcine mucosal heparin (a) and the corresponding glycol-split derivative (b) obtained by periodate oxidation and borohydride reduction of nonsulfated glucuronic (G/G') and iduronic (I) residues, to generate gsG/gsgG', and gsI [13]

LR = linkage region [23] at the “reducing” end (RE). The biochemical formula of ATBR is indicated in structure (a), starting with a residue I that is not part of the pentasaccharidic active site, but most often precedes it. Structure (a) is adapted from [22]; a major modification involves the A_{NS,6S} residue at the non-reducing end (NRE), assumed to be the consequence of cleavage (by an endo-β-D-glucosidase) of a G-A_{NS6S} glycosidic bond in the chains of the heparin proteoglycan precursor (“macromolecular heparin”). The structure of the “full” linkage region LR is reported in (c) and (d) for heparin and RO-heparin, respectively, where G_{LR} is the G residue in the LR, Gal1 and Gal2 are two galactose residues, Xyl is xylose, Ser is serine [23]. The two glycol-split residues (gsG_{LR} and gsXyl) in the LR of gs-heparin were not previously described (see text). Circled residues in the unmodified heparin structure (a) and (c) highlight unsubstituted diol groups susceptible of glycol-splitting

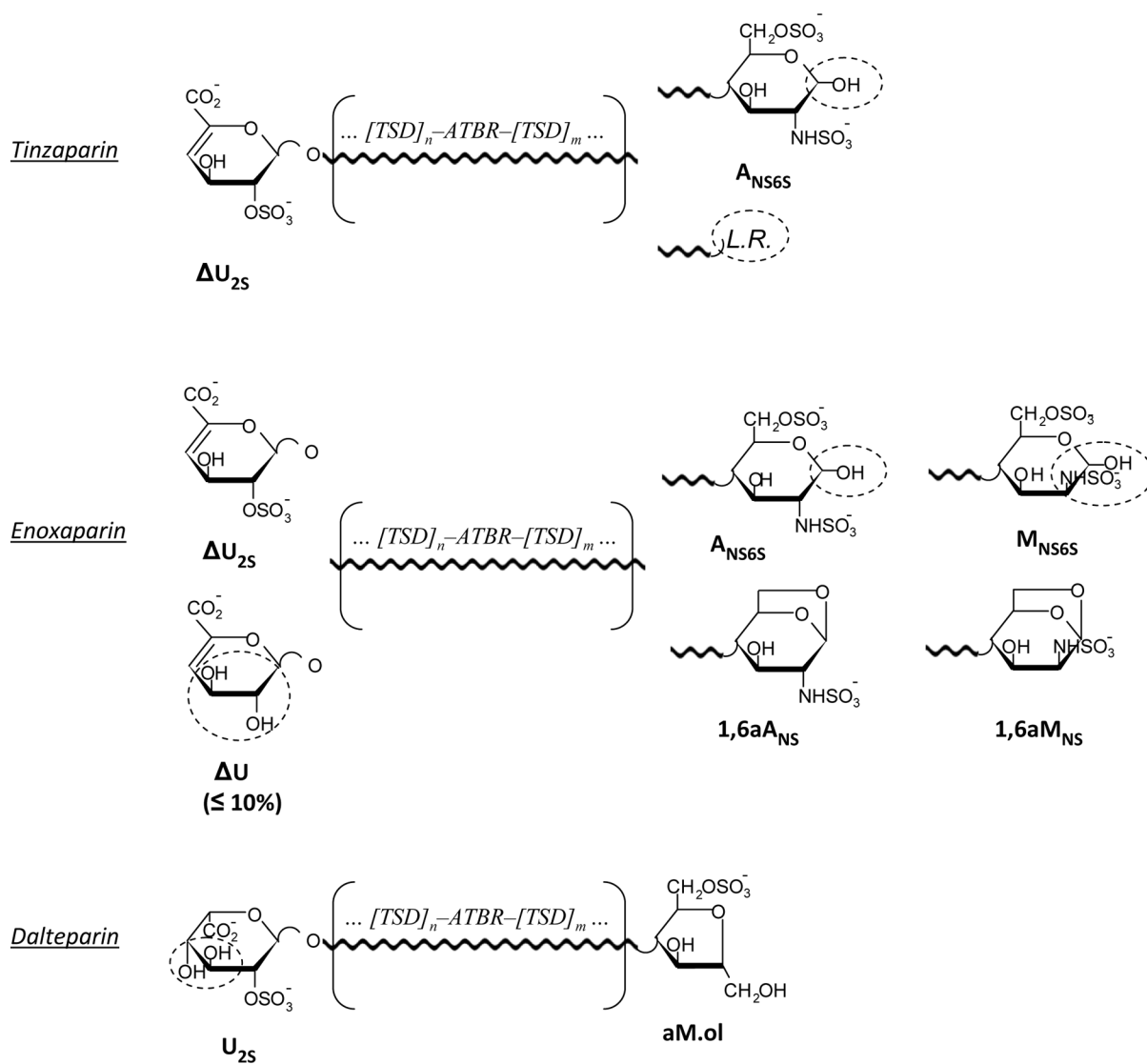


Fig. 2.
Simplified structures of tinzaparin, enoxaparin, and dalteparin
Internal sequences are indicated as substantially the same as in non-depolymerized heparin.
The end groups susceptible of being modified by periodate oxidation or borohydride reduction are circled

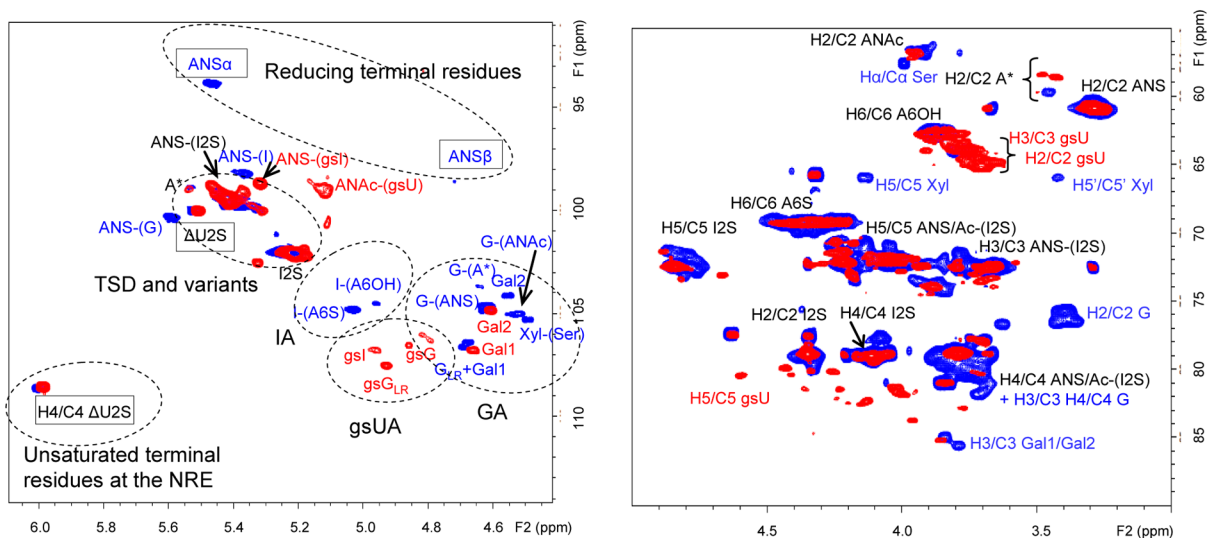
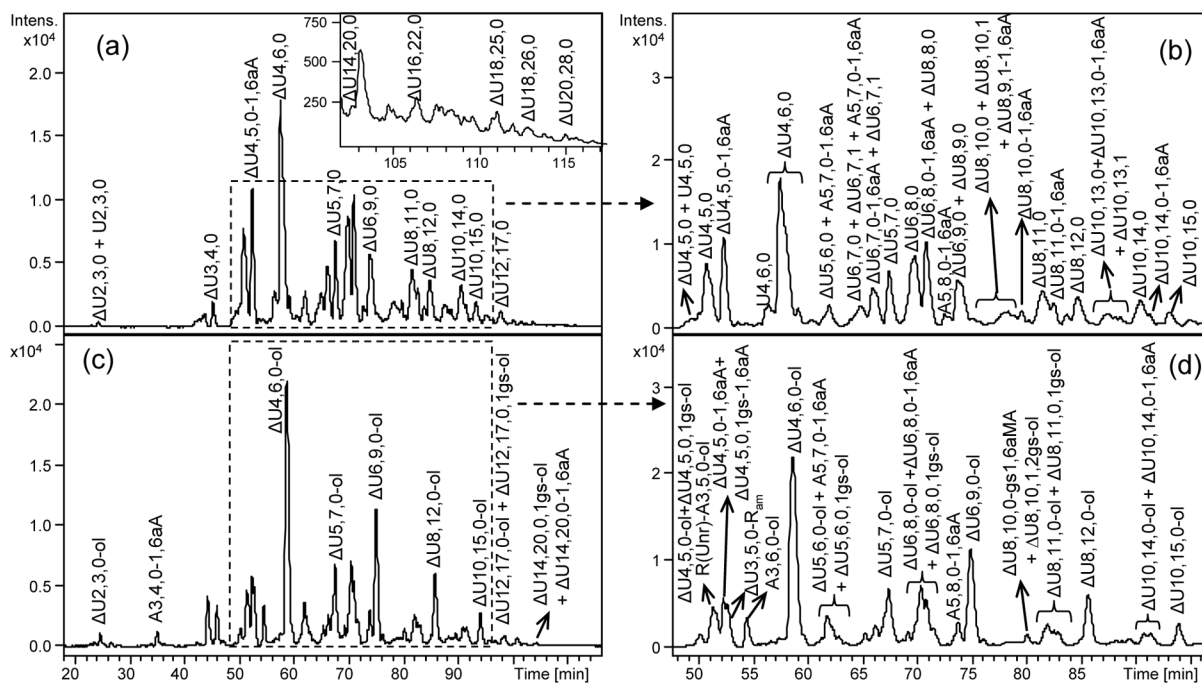


Fig. 3. Anomeric (a) and “ring” (b) regions of the $^1\text{H}/^{13}\text{C}$ HSQC NMR spectra of RO-tinzaparin (red spots) superimposed on the spectrum of the corresponding unmodified LMWH (blue spots). Symbols for typical end-group signals are framed with rectangles. A – glucosamine, A* – *N*-sulfate-glucosamine-3-*O*-sulfate, $\Delta\text{U}2\text{S}$ – 4,5-unsulfated 2-*O*-sulfated uronic acid, I/G – iduronic and glucuronic acids, G_{LR} – glucuronic acid of the linkage region sequence, gsI/gSG – glycol-split iduronic and glucuronic acids, gsU – glycol-split uronic acids, Gal – galactose, Xyl – xylose, Ser - serine

**Fig. 4.**

LC-MS profiles of enoxaparin (a), RO-enoxaparin (c) and the corresponding expanded chromatograms (b, d)

LC conditions: column C18 100 x 2.1 mm, 2.6 μ m; eluents A and B – 10 mM DBA and 10 mM CH₃COOH in H₂O-CH₃CN = 9:1 (v/v) and CH₃CN, respectively; gradient: 0 min – 0%B, 5 min – 0%B, 130 min – 35%B, 140 min – 70%B, 145 min – 70%B, 148 min – 0%B, 170 min – 0%B; flow rate – 0.25 ml/min

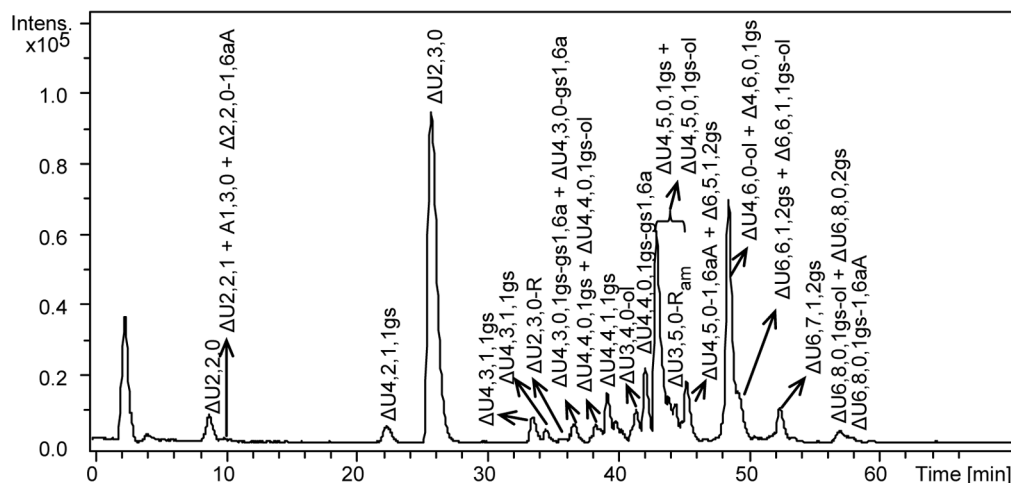


Fig. 6.

LC-MS chromatogram of the heparinase-digest of RO-enoxaparin

LC conditions: column C18 100 x 2.1 mm, 2.6 μm ; eluents A and B – 10 mM DBA and 10 mM CH_3COOH in $\text{H}_2\text{O}-\text{CH}_3\text{OH} = 9:1$ (v/v) and CH_3OH , respectively; 0 min – 17% B, 10 min – 17%B, 30 – 42%, 50 min – 50% B, 65 min – 90%, 75 min – 90%B, 76 min – 17% B, 95 min – 17 %B; flow rate – 0.1 ml/min; injection volume – 5 μl .

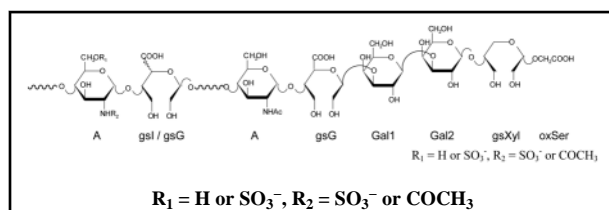
Sodium borohydride reduction was used to distinguish between internal gs-unit and alditol end residue. For example, the double-charged ion with m/z 497.02 could correspond to both $\Delta\text{U}4,4,0,1\text{gs}$ and $\Delta\text{U}4,4,0\text{-ol}$. After sodium borohydride reduction two peaks with m/z values were observed: a) m/z 498.02, indicating that this oligosaccharide containing one internal gs-unit (gsU), corresponds to the structure $\Delta\text{U}_5\text{-A}_{\text{NS}6(\text{S})}\text{-gsU-A}_{\text{NS}6(\text{S})}$, where only one of the two sulfate groups within parenthesis is present; b) unmodified m/z 497.02, which should have an internal 2-*O*-sulfated uronic acid (U_5) and corresponds to $\Delta\text{U}_5\text{-A}_{\text{NS}}\text{-U}_5\text{-A}_{\text{olNS}}$ structure. The additional NaBH_4 reduction of the RO-enoxaparin digest proved also the structure assigned to the minor tetrasaccharides terminating with an uronic acid remnant ($\Delta\text{U}4,4,1,1\text{gs-R}$, m/z 577.03 for $[\text{M}-2\text{H}]^{2-}$ ion form, and $\Delta\text{U}4,5,0,1\text{gs-R}$, m/z 596.01 for $[\text{M}-2\text{H}]^{2-}$ ion form), for which the m/z values remained constant after the additional reduction

Table 1
 Gradient used and the LMWH quantity loaded for the LC-MS profiling of the LMWHs and their RO-derivatives

Enoxaparin and RO-enoxaparin	Tinzaparin and RO-tinzaparin	Dalteparin and RO-dalteparin			
Multistep gradient					
Time (min)	% Eluent B	Time (min)	% Eluent B	Time (min)	% Eluent B
0	0	0	5	0	10
5	0	5	5	4	10
130	35	125	35	15	18
140	70	130	70	30	18
145	70	135	70	115	35
148	0	138	5	133	70
170	0	160	5	138	70
				140	10
				160	10
Sample quantity loaded, µg					
15	15	30	30	30	30
Corresponding Figure					
Fig. 4 and ESM Fig. S5		ESM Fig. S6		ESM Fig. S7	

LC conditions: column C18 100 x 2.1 mm, 2.6 µm; eluents A and B – 10 mM DBA and 10 mM CH₃COOH in H₂O-CH₃CN = 9:1 (v/v) and CH₃CN, respectively; flow rate – 0.25 ml/min

Table 2

 ^1H and ^{13}C chemical shifts in the anomeric region characteristic for the RO-LMWHs


$\text{R}_1 = \text{H or SO}_3^-, \text{R}_2 = \text{SO}_3^- \text{ or COCH}_3$

RESIDUE	^1H , ppm	^{13}C , ppm
Aminosugars		
$\text{A}_{\text{NAc}}-(\text{gsG})^a$	5.09	99.0
$\text{A}_{\text{NAc}}-(\text{gsI})^b$	5.12	98.0
$\text{A}_{\text{NS}}-(\text{gsI})^c$	5.39	99.8
$\text{A}_{\text{NS}}-(\text{R})^d$	5.34	99.2
Glycol-split uronic acids		
$\text{gsG}-(\text{A}_{\text{NAc}})^a$	4.71	106.7
$\text{gsI}-(\text{A}_{\text{NAc}})^b$	4.94	106.9
$\text{gsI}-(\text{A}_{\text{NS}})^c$	4.98	106.9
gsG (RO-heparins ^e and RO-tinzaparin)	4.87	106.4
gsG (RO-LMWHs) ^f	4.80	106.5
gsI ^e	4.98	106.9
gsU-(A*) ^g	4.90	103.2
Residues of the gsLR		
gsG-(Gal1) = gsG _{LR}	4.92	107.6
Gal1	4.66	106.9
Gal2	4.61	105.0
gsXyl	4.75	105.6

^a assignment consistent with the 2D NMR spectrum of RO-K5 (RO-derivative of N-acetylheparosan), *spectrum not shown*

^b assignment consistent with the 2D NMR spectrum of RO-derivative of N-acetylated bovine lung heparin

^c published in [14]

^d R – remnant generated by hydrolysis of glycol-split uronic acids; data obtained from 2D NMR spectrum of the fraction of heparinase-digested RO-enoxaparin, containing $\Delta\text{U}2\text{S-ANS}6\text{S}$ and $\Delta\text{U}2\text{S-ANS}6\text{S-R}$

^e reported in [13] for RO-heparins

^f present work

^g from NMR analysis of RO-dalteparin (this cross peak correlates with CH_2OH in the TOCSY spectrum indicating that it is a glycol-split uronic acid); A* = ANS3S(6S)